

# Perturbed Angular Correlation Study of the Static and Dynamic Aspects of Cadmium and Mercury Atoms Inside and Attached to a C<sub>60</sub> Fullerene Cage

Satyendra K. Das<sup>a</sup>, Rashmohan Guin<sup>a</sup>, Debasish Banerjee<sup>a</sup>, Karl Johnston<sup>b</sup>, Parnika Das<sup>c</sup>, Tilman Butz<sup>d</sup>, Vitor S. Amaral<sup>e</sup>, Joao G. Correia<sup>f</sup>, and Marcelo B. Barbosa<sup>f</sup>

<sup>a</sup> Accelerator Chemistry Section (Bhabha Atomic Research Centre), Variable Energy Cyclotron Centre, 1/AF Bidhannagar, Kolkata 700064, India

<sup>b</sup> CERN 1211 Geneva 23, Switzerland

<sup>c</sup> Variable Energy Cyclotron Centre, Kolkata 700064, India

<sup>d</sup> Faculty of Physics and Earth Sciences, University of Leipzig, Linnéstr. 5, 04103 Leipzig, Germany

<sup>e</sup> Physics Department and CICECO, University of Aveiro, 3810–193 Aveiro, Portugal

<sup>f</sup> ITN, Sacavém, Portugal and ISOLDE-CERN

Reprint requests to S. K. D.; E-mail: [satyen50@gmail.com](mailto:satyen50@gmail.com)

Z. Naturforsch. **69a**, 611–618 (2014) / DOI: 10.5560/ZNA.2014-0055

Received December 4, 2013 / revised July 26, 2014 / published online October 8, 2014

30 keV <sup>111m</sup>Cd and 50 keV <sup>199m</sup>Hg beams from ISOLDE were used to implant on preformed targets of C<sub>60</sub> with a thickness of 1 mg cm<sup>-2</sup>. Endofullerene compounds, viz. <sup>111m</sup>Cd@C<sub>60</sub> and <sup>199m</sup>Hg@C<sub>60</sub> formed during implantation were separated by filtration through micropore filter paper followed by solvent extraction. Dried samples of the endofullerene compounds were counted for the time differential perturbed angular correlation (TDPAC) measurement using the coincidence of the 151–245 keV cascade of <sup>111m</sup>Cd and the 374–158 keV cascade of <sup>199m</sup>Hg on a six LaBr<sub>3</sub>(Ce) detector system coupled with digital electronics. The results for <sup>111m</sup>Cd@C<sub>60</sub> indicate a single static component (27%) and a fast relaxing component (73%), the latter implying that the cadmium atom moves rapidly inside the cage at room temperature. The quadrupole interaction frequency and asymmetry parameter of the cadmium atom occupying the static site in C<sub>60</sub> are  $\omega_Q = 8.21(36)$  Mrad s<sup>-1</sup> and  $\eta = 0.41(9)$ , respectively. The fast relaxation constant is 0.0031(4) ns<sup>-1</sup>. Similarly, mercury atoms also exhibit a single static and a fast component. The static site has a quadrupole frequency  $\omega_Q = 283.0(12.4)$  Mrad s<sup>-1</sup> and  $\eta = 0$  with a fraction of 30%. The fast relaxation constant is 0.045(8) ns<sup>-1</sup> with a fraction of 70%, very similar to that of cadmium.

*Key words:* Endofullerene; Radioactive Ion Beam; TDPAC; Inert Pair Effect; Correlation Time.

*PACS numbers:* 61.48.+c; 61.80.-x; 76.80.+y

## 1. Introduction

After the discovery of fullerene [1], the compounds in this group which received much attention in basic research and in applications are the endofullerenes [2]. The inner diameter of the C<sub>60</sub> cage is  $\sim 4$  Å which is large enough to accommodate any atom or ion across the periodic table. The behaviour of an atom or a cluster of atoms inside the fullerene cage makes such compounds suitable for various applications in the area of superconductivity, lasers, and ferroelectric materials [3]. A very promising application of these compounds lies in its medical use [4] where the trapped

radioactive atom inside the inert carbon cage is not in direct contact with the biological system – a prerequisite for nuclear medicine. An optimistic conjecture has been made to use endofullerenes for the storage of nuclear waste by entrapping the radioactive atoms inside the cage [5, 6]. The self-healing property of C–C bonds is helpful in preserving the cage even if C–C bonds are cleaved by the radiation from radioactive atoms inside the cage. Besides the applications mentioned above, basic research interest is enormous as far as the chemical bonding of the atom inside the cage is concerned. This is the most important aspect in the study of endofullerenes.

The most well-known fullerene,  $\text{C}_{60}$ , has three degenerate lowest unoccupied molecular orbitals (LUMOs), energetically slightly above the highest occupied molecular orbitals (HOMOs) [7]. These can accommodate up to six electrons and hence, metal ions with valency up to six can be accommodated inside the cage. However, a trivalent metal ion contributing three electrons to make LUMOs half-filled stabilizes the endofullerene. Since the inner side of the cage is electrostatically slightly positively charged as the  $\pi$ -electrons of the  $sp^2$ -carbon atoms (in fullerene carbon hybridisation is  $sp^{2.27}$ ) are bulged outside, the atom inside the cage would give up electrons to fullerene to stabilize the system. The energy consideration due to the transfer of electrons between the entrapped atom and the carbon atoms of the cage thus is the decisive factor in the stabilization of the endofullerenes.

Endofullerenes are synthesised mainly through two routes: (i) simultaneous formation of fullerene in the arc vaporisation [8] or laser ablation [9] and (ii) posterior insertion of the desired atom by direct and recoil implantation [10–12] on the pre-existing fullerene. In the arc vaporisation method, a direct current (DC) arc discharge is used between two metal doped graphite electrodes. Fullerene and endofullerene formed during this discharge process are trapped and collected in a low temperature chamber. In the laser ablation method, the composite rod of graphite loaded with the desired metal is vaporised and the endofullerene and fullerene are collected at a place at lower temperature. In the process (i), thermodynamics decides the formation of the endofullerene. However, in the case of the post-insertion using implantation, the atom once entered the cage has no chance to come out. So it is only the barrier that decides the formation of the endofullerene. Once the atom enters the cage, the question remains how it behaves inside the cage. An electron paramagnetic resonance (EPR) study [13] indicates that while a nitrogen atom inside the  $\text{C}_{60}$  cage does not interact with the carbon atoms and remains in the central position of the cage, copper in  $\text{Cu@C}_{60}$  occupies a well defined (minimum potential) position inside the cage. This indicates that there is a bond of the copper atom with carbon atoms. An nuclear magnetic resonance (NMR) study [14] and the maximum entropy method (MEM)/Rietveld method [15] for imaging of diffraction data indicates that the metal atoms inside the cage rotate. A small rotational barrier in such cases can help to control the rotation by temperature.

This property of the endofullerenes can be used to develop interesting molecular devices. It is thus important to know the states of the atom inside the fullerene cage in terms of its position in the cage, charge states, dynamics etc. These parameters would be of great help to understand the mechanism of endofullerene formation which in turn would tell the route for the synthesis of the required endofullerene in significant quantities for the applications mentioned above.

Time differential perturbed angular correlation (TD-PAC), a nuclear probe technique, relies on the interaction of the nuclear quadrupole moment with the electric field gradient (EFG) produced by the surrounding charges. The angular correlation between  $\gamma$ -rays emitted in a cascade is exploited to obtain information on the electron distribution through the measurement of the EFG. The strength of the EFG and its asymmetry are the fingerprints of the electronic state of the probe atom. One thus can identify the position of the atom inside the fullerene cage with the support of theoretical calculations using e.g. density functional theory. In case there is rotation or grazing movement of the probe inside the cage, it will show up as a time-dependent perturbation of the angular correlation.

With the motivation to understand the behaviour of the atom inside the fullerene cage, we carried out the experiment starting from the synthesis of the endofullerenes  $^{111\text{m}}\text{Cd@C}_{60}$  and  $^{199\text{m}}\text{Hg@C}_{60}$ . Low energy  $^{111\text{m}}\text{Cd}$  and  $^{199\text{m}}\text{Hg}$  ion beams from ISOLDE, CERN, were used for the first time to implant on the preformed  $\text{C}_{60}$  target. After separation of the endofullerene from other products containing the  $^{111\text{m}}\text{Cd}$  and  $^{199\text{m}}\text{Hg}$  activity using a suitable chemical method described below, TDPAC measurements were carried out for the separated endofullerenes in order to investigate the static and dynamic behaviour of the atoms inside the fullerene cage. Although cadmium and mercury fall within the same group, the mercury atom, being the bottom-most element, is expected to exhibit a different behaviour from the cadmium atom because of the inert pair effect. This chemical inertness of the mercury atom and its effect on the dynamic aspect of this atom inside the fullerene cage has also been looked into with the aid of the present hyperfine tool TDPAC.

## 2. Theory

The PAC method relies on the hyperfine interaction of nuclear magnetic dipole or electric quadrupole

moments with extranuclear magnetic fields or electric field gradients. In case of electric quadrupole perturbation of the  $\gamma$ - $\gamma$  angular correlation, the coincidence measurements generate the quadrupole frequency  $\omega_Q$  along with its distribution  $\delta$  and asymmetry parameter  $\eta$  defined by  $\eta = \frac{V_{xx} - V_{yy}}{V_{zz}}$ . The TDPAC measurements were performed using the 151–245 keV  $\gamma$ - $\gamma$  cascade in  $^{111m}\text{Cd}$  after the isomeric transition (IT) decay of the  $^{111m}\text{Cd}$  parent and the 374–158 keV  $\gamma$ - $\gamma$  cascade in  $^{199m}\text{Hg}$  after the IT decay of the  $^{199m}\text{Hg}$  parent. The relevant decay schemes of these two nuclei are shown in Figure 1. The perturbation of the angular correlation function results from the interaction between the electric quadrupole moment of the intermediate nuclear level of the probe nuclei (245 keV level with  $\tau = 85$  ns and  $I = 5/2$  for  $^{111m}\text{Cd}$  and 158 keV with  $\tau = 2.45$  ns and  $I = 5/2$  for  $^{199m}\text{Hg}$ ) and the electric field gradient acting on the probe nucleus.

The nuclear quadrupole interaction (NQI) of the  $I = 5/2$  intermediate state leads to a splitting with eigenvalues [16, 17]

$$\begin{aligned} E_1 &= -2r \cos\left(\frac{\phi}{3}\right), \\ E_2 &= r \cos\left(\frac{\phi}{3}\right) - \sqrt{3}r \sin\left(\frac{\phi}{3}\right), \\ E_3 &= r \cos\left(\frac{\phi}{3}\right) + \sqrt{3}r \sin\left(\frac{\phi}{3}\right), \end{aligned}$$

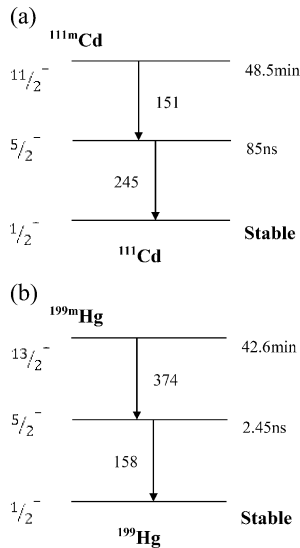


Fig. 1. (a) Decay scheme of  $^{111m}\text{Cd}$  and (b) decay scheme of  $^{199m}\text{Hg}$ .

with

$$\begin{aligned} \cos\phi &= \frac{q}{r^3}, \\ r &= \text{sign}(q)\sqrt{|p|}, \\ p &= -28\left(1 + \frac{\eta^2}{3}\right), \\ q &= -80(1 - \eta^2). \end{aligned}$$

The three precession frequencies are

$$\begin{aligned} \omega_1 &= (E_2 - E_3), \\ \omega_2 &= (E_1 - E_2), \\ \omega_3 &= (E_1 - E_3), \end{aligned}$$

where  $E_1$ ,  $E_2$ , and  $E_3$  are the three eigenvalues (in units of  $\hbar \cdot \omega_Q$ ) corresponding to the splitting of the intermediate state ( $I = 5/2$ ) of the probe due to the interaction of the quadrupole moment  $Q$  of the intermediate state with the electric field gradient tensor  $V_{zz}$  with the quadrupole frequency as

$$\omega_Q = \frac{eQV_{zz}}{40\hbar}.$$

The perturbation function is thus

$$\begin{aligned} G_2(t) &= a_0 + a_1 \cos \omega_1 t + a_2 \cos \omega_2 t \\ &\quad + a_3 \cos \omega_3 t. \end{aligned} \quad (1)$$

The experimental data were fitted with this function modified using finite distributions of  $\omega_Q$ . In the present case we have used Lorentzian distributions. The final form of the theoretical function in which the experimental data were fitted is given by

$$\begin{aligned} G_2(t) &= a_0 + \sum_{n=1}^3 a_n \exp(-\omega_n \delta t) \\ &\quad \cdot \exp\left(-\frac{1}{2} \omega_n^2 \tau^2\right) \cos(\omega_n t). \end{aligned} \quad (2)$$

The exponential terms account for the finite resolving time characterized by a Gaussian distribution with standard deviation  $\tau$  and the Lorentzian frequency distribution with relative width parameter  $\delta$ . The coefficients  $a_n$  depend on the nuclear spin and the asymmetry parameter.

When the electric field fluctuates in magnitude and direction, it gives rise to a time-dependent EFG since the quantization axis undergoes constant change. This

fluctuating electric field is described by a parameter called the correlation time  $\tau_c$  which signifies the time separating two different interactions between the nuclear quadrupole moment and the EFG. In case of isotropic fluctuations fast enough to fulfil both conditions  $\tau_c \ll \tau$  and  $\tau_c \ll \frac{2\pi}{\omega_0}$ , the Abragam–Pound theory [18] leads to an exponential attenuation factor

$$G_k(t) = \exp(-\lambda_k t), \quad (3)$$

where the relaxation constant is described by the following equation:

$$\lambda_k = \frac{3}{80} \left( \frac{eQ}{\hbar} \right)^2 \langle V_{zz}^2 \rangle \tau_c k(k+1) \cdot \left[ \frac{4I(I+1) - k(k+1)}{I^2(2I-1)^2} \right]. \quad (4)$$

For the intermediate  $I = 5/2$  state, the relaxation constant (in addition to  $\lambda_0 = 0$ ) takes the form

$$\begin{aligned} \lambda_2 &= 0.063 \left( \frac{eQ}{\hbar} \right)^2 \langle V_{zz}^2 \rangle \tau_c \\ &= 100.8 \langle \omega_Q^2 \rangle \tau_c. \end{aligned} \quad (5)$$

The correlation time reflects the dynamic behaviour of the atom inside the fullerene cage. A smaller correlation time signifies a faster movement of the atom inside the cage and vice versa. This aspect has been investigated in our present study.

### 3. Experimental

$\text{C}_{60}$  targets were prepared on  $10 \times 8 \text{ mm}^2$  Whatman-42 filter paper by soaking the toluene solution of  $\text{C}_{60}$  on the filter paper mentioned above and subsequently drying the filter paper. The target amount was approximately  $1 \text{ mg cm}^{-2}$ . A 30 keV beam of  $^{111\text{m}}\text{Cd}$  and a 50 keV beam of  $^{199\text{m}}\text{Hg}$  available from ISOLDE were implanted into the  $\text{C}_{60}$  target to prepare  $^{111\text{m}}\text{Cd}@\text{C}_{60}$  and  $^{199\text{m}}\text{Hg}@\text{C}_{60}$  endofullerenes in two separate experiments. The beam current was  $\sim 10^9$  ions  $\text{s}^{-1}$ . Total fluxes of ions collected were  $3 \times 10^{12}$  ions for different samples. Six irradiations were carried out for each ion. The irradiated fullerene target was treated with toluene to dissolve the fullerene from the filter paper. Any decomposed products of fullerene formed due to the irradiation of fullerene with energetic ions were removed by micron filter paper (pore size is

0.5 micron). This filter paper contained a large amount of radioactivity and only a small fraction of the order of 1% was available in the filtered solution. This filtered solution was treated for the solvent extraction with 6 M HCl solution to remove the  $^{111\text{m}}\text{Cd}$  or  $^{199\text{m}}\text{Hg}$  attached to the fullerene exohedrally or the ions attached outside the  $\text{C}_{60}$  cage. The atoms attached to the exo products are expected to dissolve in 6 M HCl [10]. However the atoms trapped inside the cage are shielded by the inert carbon atoms and are unaffected by the acid and thus the endofullerene products remain in the organic phase. The toluene fraction thus contains only the endofullerenes alongwith pure fullerene molecules. Toluene was evaporated to get the dried endofullerene fraction which was then counted on the TDPAC setup [19] consisting of six  $\text{LaBr}_3(\text{Ce})$  detectors coupled to digital electronics.  $^{111\text{m}}\text{Cd}$  ( $t_{1/2} = 49\text{m}$ ) and  $^{199\text{m}}\text{Hg}$  ( $t_{1/2} = 43\text{m}$ ) have similar half lives. Each sample was counted for three hours, i.e. nearly four half lives of the parent nucleus.

### 4. Results and Discussion

It is important to know whether the endofullerene is formed in the present experimental condition and to what extent. Mass spectrometry or high performance liquid chromatography (HPLC) is used for this purpose, in general (references in [2]). HPLC is also used for the purification of the fullerene products. However, the chemical separation methodology [11] can also justify the formation of endofullerenes. In our previous work [10], we argued that the organic solvent contains the fullerene and endofullerene products as the radioactivity attached externally to fullerene molecules are dissolved in strong acid and remain in the aqueous phase after solvent extraction. Our strong point of argument was the case for the endofullerene formed by  $^{79}\text{Kr}$ . The presence of radioactivity only in the organic phase containing the fullerenes (both pure and endofullerenes have solubility in the organic phase) is a clear indication of the formation of  $^{79}\text{Kr}@\text{C}_{60}$  as krypton is an inert gas atom which does not form any compound with fullerene molecules except being trapped inside the fullerene cage to form an endofullerene.

In this present work also, we propose the same argument in favour of the formation of endofullerenes. Thus it can be safely assumed that endofullerenes are formed in the present experimental condition. It was

found that the activity of either  $^{111m}\text{Cd}$  or  $^{199m}\text{Hg}$  in the chemically separated toluene fraction of endofullerene was two orders of magnitude less than the irradiated sample before chemical separation. In other words, the yield of endofullerene is less than one percent. Most of the radioactivity was found in the filter paper used for the separation of the decomposed products of fullerene suspended in toluene. Energetic  $^{111m}\text{Cd}$  or  $^{199m}\text{Hg}$  ion beams, when interacting with fullerene, lose their energy and when the energy reaches a few tens of eV (barrier for entrance inside the cage), the ions open up the hexagon ring and get trapped inside the cage. These probes trapped inside the cage convert fullerene to endofullerene. The probe atom inside the cage may or may not move/graze inside the fullerene cage. This depends on the potential surface of the inner surface of the cage for the probe atoms at a particular temperature. The atom not moving inside the cage experiences a static interaction. However, the probe moving inside the cage experiences a time-dependent interaction with fluctuating EFG. This gives rise to the dynamic component described below. No other species of fullerene can give rise to such dynamic behaviour of the probes. This is also an indication in favour of the formation of endofullerene. During the process of energy loss there is also a damage of fullerene molecules which may agglomerate to bigger size and suspend in the toluene medium. During this process, some cadmium and mercury ions get trapped in the agglomerates of the dam-

aged fullerene molecules. These are separated by the micropore filter paper. Thus the toluene fraction after solvent extraction is expected to contain only the endofullerene part along with pure fullerene molecules. It should be mentioned here that HPLC [2] would have been desirable in the present work to separate the endofullerene from the pure fullerene molecules. However, due to rather low yield and the short half-lives of the probe atoms this was not considered feasible.

Figure 2 shows the TDPAC spectrum for the  $^{111m}\text{Cd}@C_{60}$  endofullerene and Figure 3 shows that for the  $^{199m}\text{Hg}@C_{60}$ . The data are fitted with a static interaction as mentioned in (1) and a time-dependent part mentioned in (3). The uppermost panel of Figures 2 and 3 are the total spectrum which is split into the static and the dynamic parts, as mentioned above. The static part is illustrated in the middle panel and the dynamic part in the bottom panel. Fitting has been performed using the code WINFIT version 3.0.4 [20] developed at Leipzig University. It is seen that the TDPAC spectra for both  $^{199m}\text{Hg}@C_{60}$  and  $^{111m}\text{Cd}@C_{60}$  could be fitted with one static and a time-dependent interaction. To understand the dynamic component in the hyperfine interaction it would be helpful to have temperature dependent data in order to distinguish between a dynamic part and a static inhomogeneous broadening unless we see that the anisotropy vanishes at long time. This is approximately the case for  $^{199m}\text{Hg}@C_{60}$ , thus we can exclude the possibility of

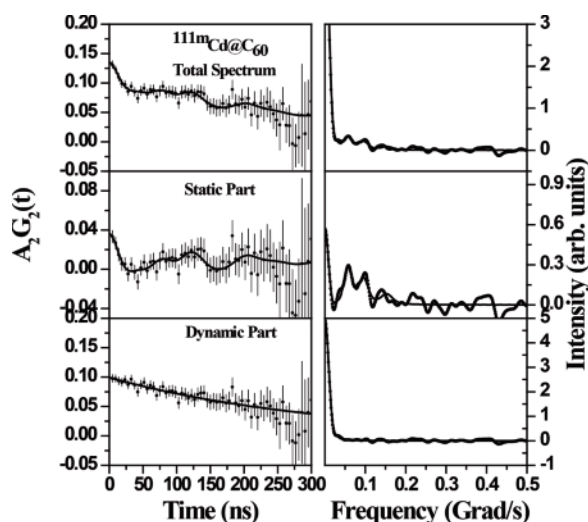


Fig. 2. TDPAC spectrum for the  $^{111m}\text{Cd}@C_{60}$  endofullerene (left) and the corresponding Fourier spectrum (right).

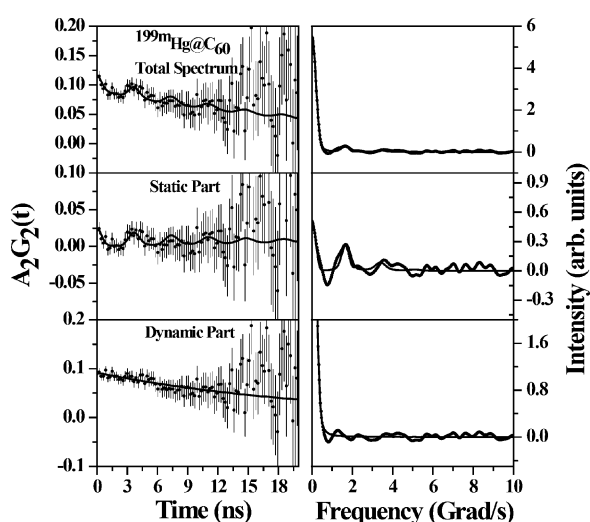


Fig. 3. TDPAC spectrum for the  $^{199m}\text{Hg}@C_{60}$  endofullerene (left) and the corresponding Fourier spectrum (right).

Sample	$\omega_Q$ (Mrad s $^{-1}$ )	$\eta$	$\delta$ (%)	Fast $\lambda$ (ns $^{-1}$ )	Population (%)	
					Static	Dynamic
$^{111\text{m}}\text{Cd}$	8.21(36)	0.41(9)	7.7(4.7)	0.0031(2)	27(3)	73(2)
$^{199\text{m}}\text{Hg}$	283.0(12.4)	0.0(0)	5.2(6)	0.045(8)	30(11)	70(1)

Table 1. TDPAC results for the products formed by  $^{111\text{m}}\text{Cd}$  and  $^{180\text{m}}\text{Hg}$  probes with fullerene.

a very broad static component. For  $^{111\text{m}}\text{Cd}@C_{60}$  this is not the case. Therefore we analysed the data with a static broad component along with a much sharper static component. The same data were then analysed with one static and a dynamic component. As far as the  $\chi^2$  of the fitting is concerned, it is difficult to distinguish between the two situations. However, when a broad static component was chosen, the fit required an unphysically high baseline shift. Based on this analysis it is justified to accept the presence of the dynamic component along with a static part for both probes used in this experiment. Table 1 shows the TDPAC results obtained by fitting the spectra for both probes. The last column of the table shows the fraction of these two components. It is seen that for both probes the static part has a fraction of about 30%, and the remaining 70% is due to fast relaxation caused by the fluctuating EFG experienced by the probe nucleus. This is expected because the two probes are from the same group of the periodic table and have a similar chemical behaviour. Therefore the distribution of the atoms in these two compounds is expected to be similar. The origin of this fluctuation in the EFG is expected to arise from the movement of the probe atoms inside the cage.

Now the question is how both static and dynamic interaction can exist at the same time for these probes. It would be difficult to assume that atoms inside the cage can lead to both static and dynamic interactions. The only reason could be that when cadmium and mercury ion beams interact with  $C_{60}$ , they cause damage in the  $C_{60}$  molecules [21] and during this process the metal atoms may be trapped in a cluster of damaged  $C_{60}$  molecules. The bigger agglomerates are separated by the micropore filter paper which contains almost 99% of the total activity of the probes. However, a fraction of these clusters which are smaller in dimension might not be separated by the filter papers and remain suspended in toluene even after filtration. These are not the exohedral products. The reason has been explained above. It should be mentioned here that in this work, we have not carried out any specific experiment to physically separate the species responsible for the static and dynamic interactions we resolved from the

TDPAC data. However, the analysis of data has clearly separated these two species for both the probes. One may have a doubt whether the observation has an origin other than the fullerene compounds. It should be noted here that the thickness of the fullerene target was adequate to stop the ion beams used in this experiment. It is thus concluded that the observations pertain to the fullerene compounds only. The analysis indicates the unique nature of species formed by both the probes.

An indication of the nature of species is mentioned below on the basis of the TDPAC parameters. These small clusters entrapping the probe atoms could give rise to the static fraction of the hyperfine interaction. One static component with a definite value of  $\omega_Q$  and  $\eta$  indicates that the probes form a definite bond with carbon atoms of the fullerene molecule. The high value of  $\omega_Q$  and  $\eta=0$  for  $^{199\text{m}}\text{Hg}@C_{60}$  suggests to assume a twofold coordination of mercury with carbon atoms [22] similar to the compound of mercury viz.  $\text{Hg}(\text{CH}_3)_2$  which has a frequency value of 377 Mrad s $^{-1}$  ( $\omega_Q$ ) higher than 283 Mrad s $^{-1}$  observed in the present study. Of course, in the  $\text{Hg}(\text{CH}_3)_2$  molecule,  $\text{CH}_3$  ligands are different than the bonding in endofullerene. Other examples of twofold coordinations are S–Hg–S-bonds [23, 24] in  $\text{HgS}_2$  or bonds in  $\text{HgO}$  [25]. The same carbon coordinated compound of cadmium viz.  $\text{Cd}(\text{CH}_3)_2$  has a frequency value 150 Mrad s $^{-1}$  [22] much higher than the present value for the endofullerene compound. As in the case of mercury, cadmium also has a different coordination in the methyl compound than in endofullerene. Considering the low quadrupole frequency and the inter-

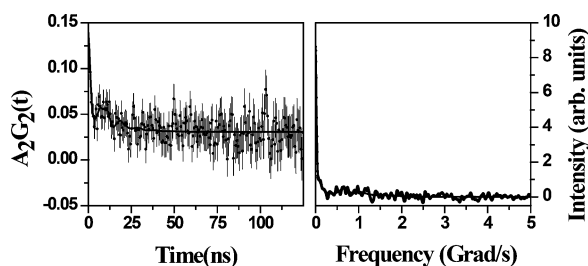


Fig. 4. TDPAC spectrum for the  $C_{60}$  decomposition products on the filter paper (left) and the corresponding Fourier spectrum (right).



mediate value of the asymmetry parameter, we propose a distorted tetrahedral structure of the compound formed by cadmium with carbon atoms. The dynamic fraction is expected due to the movement of the metal atoms inside the cage of  $\text{C}_{60}$ . This is possible when the potential on the inner surface of  $\text{C}_{60}$  is relatively flat indicating no preferred place where cadmium or mercury can attach at room temperature.

A similar situation has been observed in case of  $\text{La}_2@C_{80}$  [26]. Since  $\lambda_2 \propto \langle \omega_Q^2 \rangle \tau_c$ , it follows that  $\tau_c$  for mercury is 80 times smaller in magnitude than that for cadmium assuming their experimental  $\omega_Q$ -values of the static components. This is rather speculative because there is no knowledge of the static parameters of the probes inside the cage. A comparison of the rate of relaxation between cadmium and mercury shows a faster movement of mercury than cadmium despite mercury being heavier than cadmium. The reason is that mercury exhibits an inert pair effect and the  $s$ -electrons of mercury have much less affinity to interact with the carbon atoms of  $\text{C}_{60}$ . This makes mercury more loosely bound and thus has a faster motion as indicated by the higher relaxation constant  $\lambda_2$ . Theoretical calculations in the line of mapping the potential of the metal atom on the inner surface of  $\text{C}_{60}$  are in progress to corroborate the experimental results for the endofullerene.

To check the nature of products formed by the energetic ions with  $\text{C}_{60}$ , a typical sample of the filter paper along with the damaged products of fullerene was measured. The results were very different, as shown in Figure 4. The wide frequency distribution indicates that the products do not have a well-defined structure. This is actually a mixture of the products containing the probe nuclei at a variety of sites in the damaged fullerene which is expected to show a broad frequency distribution.

## 5. Summary and Outlook

Energetic beams of nuclear probes, viz.  $^{111m}\text{Cd}$  and  $^{199m}\text{Hg}$ , were implanted into preformed  $\text{C}_{60}$  targets to produce the respective endofullerenes  $^{111m}\text{Cd}@C_{60}$  and  $^{199m}\text{Hg}@C_{60}$ . They were separated from other products by chemical methods. The TDPAC data of the endofullerene components indicate that in both cases there exist time-dependent components of the hyperfine interaction. This shows that both cadmium and mercury atoms move inside the fullerene cage but with different speed. A faster motion of the mercury atom compared to that of cadmium is presumably due to the fact that mercury exhibits an inert pair effect causing weaker interaction of mercury with the carbon atoms than that of cadmium atoms. The static part of the TDPAC spectrum possibly arises from specific decomposition products of fullerenes to which the probe nuclei attach. The measurement at different temperatures would be interesting to see the change in the motion of the atoms inside the fullerene cage. Further work on this line is in progress.

### Acknowledgement

The authors sincerely thank all the ISOLDE crew members who were engaged in giving ion beams of  $^{111m}\text{Cd}$  and  $^{199m}\text{Hg}$ . The authors also thank the ISOLDE group for providing funds to us to carry out the experiment at ISOLDE. Some of us (S.K.D., R.G., D.B.) sincerely thank Dr. K.L. Ramkumar, Director, Radiochemistry and Isotope Group and Dr. A. Goswami, Head, Radiochemistry Division, BARC for their keen interest in this work. One of us (P.D.) sincerely thank Dr. D.K. Srivastava, Director, VECC for his keen interest in the work.

- [1] W. Kroto, J. R. Heath, S. C. O. Brien, and R. R. Curi, R. E. Smalley, *Nature* **318**, 165 (1985).
- [2] H. Shinohara, *Rep. Prog. Phys.* **63**, 843 (2000).
- [3] D. S. Bethune, R. D. Johnson, J. R. Salem, M. S. de Vries, and C. S. Yannoni, *Nature* **366**, 123 (1993).
- [4] T. Braun (Ed.), *Developments in Fullerene Science, Nuclear and Radiation Chemical Approaches to Fullerene Science*, Vol. 1, Kluwer Academic Publishers, Dordrecht, The Netherlands 2000.
- [5] T. Guo, M. D. Diener, Y. Chai, M. J. Alford, R. E. Haufler, S. M. McClure, T. Ohno, J. H. Weaver, G. E. Scuseria, and R. E. Smalley, *Science* **257**, 1661 (1992).
- [6] D. I. Koruga, U. S. Patent US005640705A (1997).
- [7] R. C. Haddon, L. E. Brus, and K. Raghavachari, *Chem. Phys. Lett.* **125**, 459 (1986).
- [8] W. Kraetschmer, K. Fostiropoulos, and D. R. Huffman, *Chem. Phys. Lett.* **170**, 167 (1990).

- [9] W. Kraetschmer, K. Fostiropoulos, L. D. Lamb, and D. R. Huffman, *Nature* **347**, 354 (1990).
- [10] S. K. Saha, D. P. Choudhury, S. K. Das, and R. Guin, *Nucl. Instrum. Methods* **243**, 277 (2006).
- [11] T. Braun and H. Rausch, *Chem. Phys. Lett.* **288**, 179 (1998).
- [12] T. Ohtsuki, H. Youki, M. Muto, J. Kassagi, and K. Ohno, *Phys. Rev. Lett.* **93**, 112502 (2004).
- [13] C. Knapp, N. Weiden, and K. Peter Dinse, *Magn. Reson. Chem.* **43**, (2005) 199.
- [14] T. Akasaka, S. Nagase, K. Kobayashi, M. Waelchli, K. Yamamoto, H. Funasaka, M. Kako, T. Hoshino, and T. Erata, *Angew. Chem. Int. Ed. Engl.* **36**, 1643 (1997).
- [15] M. Takata, E. Nishibori, M. Sakata, and H. Shinohara, *Struct. Bond.* **109**, 59 (2004).
- [16] T. Butz, *Hyperfine Interact.* **52**, 189 (1989).
- [17] T. Butz, *Hyperfine Interact.* **73**, 387 (1992) (Erratum to [16]).
- [18] A. Abragam and R. V. Pound, *Phys. Rev.* **92**, 943 (1953).
- [19] M. Jäger, K. Iwig, and T. Butz, *Hyperfine Interact.* **198**, 167 (2010).
- [20] F. Heinrich and T. Butz, <http://uni.leipzig/~nfp>.
- [21] J. Kastner and L. Palmetshofer, *Fullerene Sci. Techn.* **4**, 179 (1996).
- [22] H. Haas and D. A. Shirley, *J. Chem. Phys.* **58**, 3339 (1973).
- [23] T. Butz, W. Tröger, T. Pöhlmann, and O. Nuyken, *Hyperfine Interact.* **80**, 1121 (1993).
- [24] T. Butz, *Hyperfine Interact.* **80**, 1079 (1993).
- [25] T. Butz, A. Lerf, and R. Huber, *Phys. Rev. Lett.* **48**, 890 (1982).
- [26] K. Kobayashi, S. Nagase, and T. Akasaka, *Chem. Phys. Lett.* **261**, 502 (1996).